



Principles of a Defect Localisation in Nonlinear Ultrasonic Mixing Impulse Spectroscopy

K. Hajek* and V. Nenakhova

Department of Electrical Engineering, University of Defence, Brno, Czech Republic

The manuscript was received on 3 March 2014 and was accepted after revision for publication on 2 December 2014.

Abstract:

Principles of nonlinear ultrasonic mixing impulse spectroscopy (NUMIS) show great potential advantages in comparison with other nonlinear ultrasonic methods. It is first of all from the point of view of sensitivity and possibility of quick, simple and precise localization of a defect. This paper elaborates on the principles and algorithms of calculation of the defect place for this method. The point idealization of ultrasonic transducers and receivers are supposed for this aim. With the successive increase in delay of the second excitation pulse to the first one it can be obtained distribution of image defects on test subjects in a 2D plane within seconds.

Keywords:

nonlinear ultrasonic mixing spectroscopy, sensitivity, impulse excitation, localization.

1. Introduction

The non-linear ultrasonic spectroscopy is developed in order to obtain more appropriate methods in comparison with conventional ultrasonic methods. Specifically, the goal is to achieve a particularly high sensitivity to small defects, less sensitivity to parasitic reflections of the ultrasonic signal and capabilities for complex shapes of test objects [1].

These nonlinear methods are considered in different directions; mainly this is for case with one [2], two or more excitation signals, excitation by continuous signal or by impulse signal. The most published method uses the modulation principle [3-6]. The Time-Reversal method is considered as the most progressive in this time [7].

Published results show that these methods did not achieve expected results, mainly in terms of higher sensitivity and accuracy of localization. These problems were analysed in [8] and different principles were compared. This paper shows advantages of the mixing methods to enable effective analog pre-filtration and due to this increasing

* Corresponding author: Faculty of Military technologies, University of Defence, Kounicova 65, CZ-612 00 Brno, Czech Republic, phone: +420 730 614 120, E-mail: karel.hajek@unob.cz

dynamic range and sensitivity of the method. The basic block diagram of this method is shown in Fig. 1.

The main idea consists in sending two impulses (bursts) with harmonic signals with different frequencies f_1 and f_2 , (see Fig. 2). These bursts are mutually time-shifted in successive steps. When two waves come across in the place of defect with nonlinear properties, the new frequency component with different frequency f_d will be created. The example with exciting frequencies $f_1 = 1.5$ MHz and $f_2 = 1$ MHz and the difference frequency $f_d = 500$ kHz was shown in [8]. This choice of the frequency values fulfils two aims. It enables the use of sufficient analog pre-filtration, and it also allows the sufficiently precise localization because the high of difference frequency corresponds to a short wavelength.

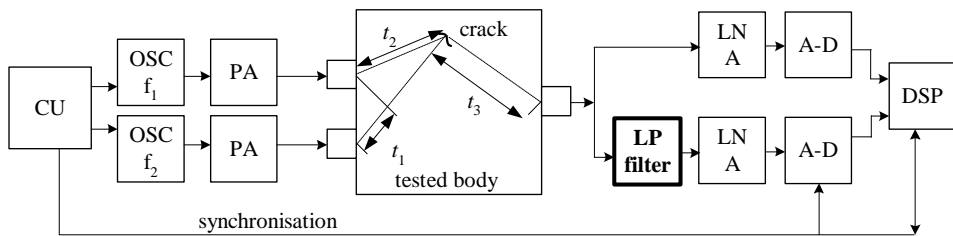


Fig. 1 Principal block diagram of nonlinear ultrasonic mixing impulse spectroscopic method [8] (CU – control unit, OSC- oscillator, PA - power amplifier, LNA – low noise amplifier, DSP – digital signal processing).

Further analysis of the principles of this method showed the need for detailed analysis of time and geometry of spaced ultrasonic transmitters and receivers on the tested object (considered 2D plane). Following this, it is necessary to derive adequate ways of computing the coordinates of the defect for the purposes of localization, which is the subject of this article.

2. Geometric and Time Relations at Localization System

Basic of geometric lay-out in 2D plane with dotted simplification of the places of ultrasonic receivers and transmitters is shown in Fig. 2. Two transmitters for sending ultrasonic signals are located in points T_1 and T_2 . In comparison with first article [8] there are considered two ultrasonic receivers R_1 and R_2 because one receiver cannot allow the explicit localization of the defect place.

For simplicity, the geometric sizes were normalized so that transmitters T_1 and T_2 are located on x-axis in points -1 and 1 . This normalised distance 2 corresponds to the time t_{T12} of the ultrasound propagation between these places (Fig. 2). As it was mentioned, the main principle of this method consists in sending two burst signals from two transmitters with different frequencies with delay t_D of the impulse T_1 in comparison with T_2 . This delay can be normalized according to ratio

$$2a = \frac{t_D}{t_{T12}/2}, \quad (1)$$

see Fig. 2 and Fig. 3 a, b. A geometric place of the encounter of both waves will create hyperbola h , as shown in Fig. 2. Focus of this hyperbola is in the point of transmitter T_1 (normalized coordinate -1) and half-axis a . In case of the reverse mutual time shift

between transmitters T_1 and T_2 , the solution will be second hyperbola branch in the right half plane and it will be in total symmetry to the first solution.

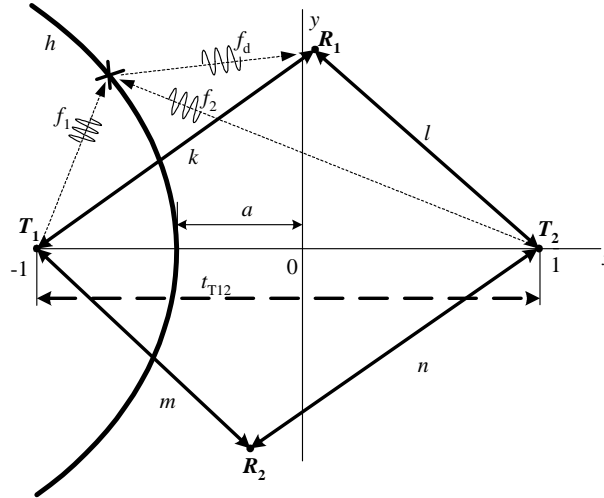


Fig. 2 Basic normalized geometrical relations between ultrasonic transmitters and receivers

Further, it is necessary to express the receiver coordinates of point R_1 and R_2 . They can be found by measuring the time of ultrasonic propagation from transmitters to receivers. The corresponding intervals k , l , m , n can be obtained by normalization of these time intervals by $t_{T12}/2$. The normalized coordinates of both receivers can be obtained from the normalized transmitters coordinates $(-1; 0)$ and $(1; 0)$ and normalized lengths k , l , m , n .

3. Geometric Analysis and Time Ratio for the Focus Point

Now, let us consider two waves come across at the defect place on this hyperbola. Nonlinear property of this defect causes that this point becomes a source of ultrasonic signal with different frequency f_d and this new signal will radiate to all directions. Then we will measure beginnings of this pulse with the intermodulation frequency f_d by receivers R_1 and R_2 after the corresponding times of propagation, as it is visible in Fig. 2 and as it is shown in the timeline of Fig. 3 c) and d). With a view from receiver R_1 , the potential places of the defect points D_{1a} and D_{2a} are shown in Fig. 4 a). It is obvious that it is sufficient to consider the time of signal propagation from transmitter T_1 to receiver R_1 , which corresponds to the normalized length $k_z = k_1 + k_2$ in Fig. 3 c). This is based on the consideration that a time delay between signals from transmitters T_1 and T_2 will always correspond to normalized delay $2a$ for the location of a potential defect on hyperbola h . Furthermore, the normalized time shift k_z can be expressed by the inequality

$$k_z = k_1 + k_2 \geq k \quad (2)$$

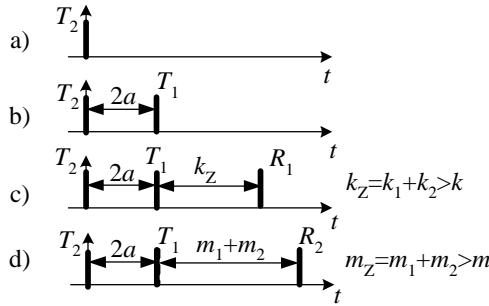


Fig. 3 Time relations between transmitted and received signals.

In case $k_Z = k$, the place of defect is located in the crossing of the line T_1R_1 and hyperbola h . If $k_Z > k$, the geometric place of potential defects corresponds to ellipse e_1 with foci T_1 and R_1 . The points of the potential defects D_{1a} and D_{1b} have to be on the crossing of ellipse e_1 and hyperbola h . Time of signal propagation through points D_{1a} respectively D_{1b} is the same from both transmitters T_1 and T_2 ($k_{1a} + k_{2a} = k_{1b} + k_{2b}$, $k_{T21} + k_{2a} = k_{T22} + k_{2b}$), see Fig. 4 a.

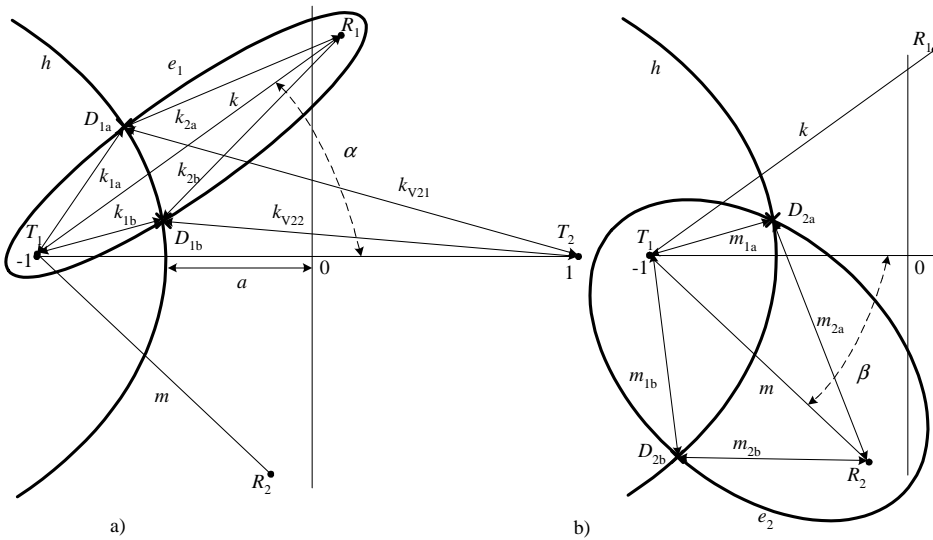


Fig. 4 Normalized geometrical relations for potential places of defects:
 a) solution for receiver R_1 , b) solution for receiver R_2

Analogically we can obtain a solution of the potential defect places D_{2a} respectively D_{2b} from the view of receiver R_2 , as it is shown in Fig. 4 b). In this case, time of signal propagation from transmitter T_1 to receiver R_2 is the interval $m_z = m_1 + m_2$ (Fig. 3d) and this interval must be equal to or greater than minimum propagation interval m . Analogically, the geometric place of potential defects corresponds to ellipse e_2 with foci T_1 and R_2 and potential defects D_{2a} and D_{2b} are on the crossing of this ellipse e_2 and hyperbola h .

The final location of the real defect place has the solution which corresponds to two cases for the propagation of signal to receivers R_1 and R_2 (Fig. 3 c, d). If both wave edges

come across at the defect place, there is only one solution, which corresponds to intersection of both above-discussed solutions for receivers R_1 and R_2 . The case from Fig. 4 shows that result solution is point $D_{1b} \equiv D_{2a}$ as intersection of both partial solutions.

Because the exciting impulses are not extremely short, we cannot exclude the situation when the front of first wave (T_1) meets with the other later waves from the second impulse (T_2) in the place of the defect. In this case the place of the defect is not in curve of corresponding hyperbola h and above expressed conditions will not apply and the defect places will not be found as an intersection for the both receivers.

4. Finding Coordinates of Potential Defect Place D_a and D_b .

As input data there are used normalized intervals between detached sensors (k, l, m, n), normalized time shift $2a$ between both exciting signals and measured intervals k_z or m_z (Fig. 3 c, d). The angle α of rotation ellipse e_1 (Fig. 6) can be expressed from appropriation law of cosine

$$\alpha = \arccos \frac{4 + k^2 - l^2}{4k}. \quad (3)$$

Normalized values of the hyperbola parameters are defined as $e_h = 1$ and $a_h = a$. Parameters of the ellipse can be expressed by equations

$$e_e = k/2, \quad (4)$$

$$a_e = k_z/2 \quad (5)$$

The core of the solution is looking for the coordinates of crossing points between hyperbola and ellipse. Because the hyperbola and ellipse have one joint point and the main axis of the ellipse is rotated by an angle (Fig. 4 a and Fig. 6), it is suitable to use polar coordinates for formulation of the ellipse and hyperbola. The ellipse (Fig. 5 a) can be described by equation

$$r_e = \frac{b_e^2}{a_e - e_e \cos \varphi_e} = \frac{a_e^2 - e_e^2}{a_e - e_e \cos \varphi_e}, \quad (6)$$

the hyperbola (Fig. 5 b) can be expressed by equation

$$r_h = \frac{b_h^2}{a_h + e_h \cos \varphi_h} = \frac{a_h^2 - e_h^2}{a_h + e_h \cos \varphi_h} = \frac{a_h^2 - 1}{a_h + \cos \varphi_h}, \quad (7)$$

where $e_h = 1$ in our model.

If we consider the simple case with non-rotated ellipse, the crossing points are defined by conditions $r_e = r_h$ and $\varphi_e = \varphi_h$. The phase φ can be expressed by equation (3) and (4) as

$$\varphi = \arccos \frac{a_e(1 - a_h^2) - a_h(a_e^2 - e_e^2)}{a_e^2 - e_e^2 + a_e(1 - a_h^2)}. \quad (8)$$

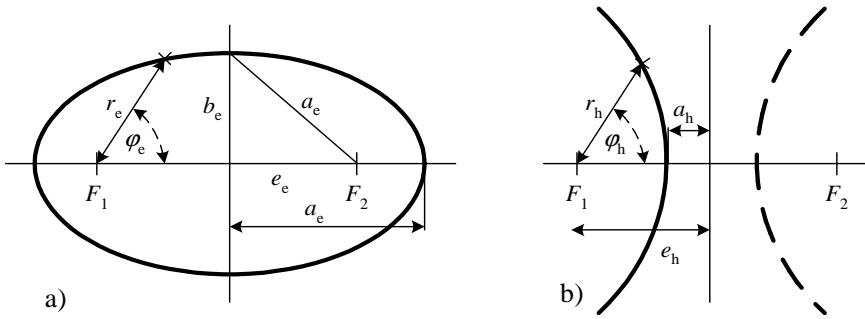


Fig. 5 Basic description of ellipse and hyperbola

The angle shift α of rotated ellipse according to Fig. 6 changes the equation (6) to form

$$r_e = \frac{a_e^2 - e_e^2}{a_e - e_e \cos(\varphi_h - \alpha)} \tag{9}$$

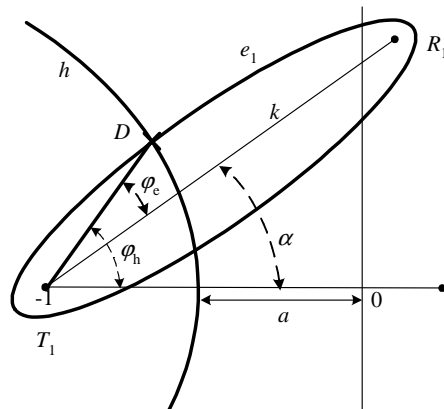


Fig. 6 Definition of angles for solution of intersection of hyperbola and ellipse

In this case the set of equations (4) and (6) does not have a simple, explicit solution and that is why a numerical solution was used for φ within the interval $(-\pi, \pi)$.

The algorithm was designed and verified in Matlab program for this kind of solution. One example is used for demonstration of this solution. We used the following input values: $\alpha = 60^\circ$, $a_e = 1$, $e_e = 0.9$ and $a_h = 0.5$. The result of this algorithm with the crossing points of the ellipse and hyperbola is shown in Fig. 7.

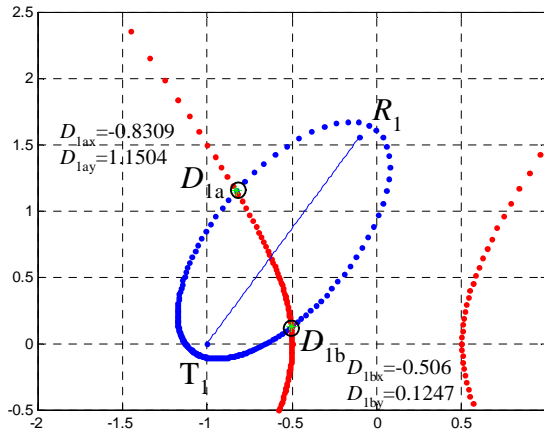


Fig. 7 Example solution of intersections of the hyperbola and shifted ellipse for $\alpha = 60^\circ$, $a_e = 1$, $e_e = 0.9$ and $a_h = 0.5$

5. Conclusion

The article shows the principles and computation algorithm for solution of the defect place for the new method which is based on nonlinear ultrasonic mixing impulse spectroscopy. This method should be more sensitive and should offer an easier way of localization the defect place in comparison with other nonlinear ultrasonic methods.

It is important to note, that this solution was derived from simplified conditions as dotted sources of the ultrasonic signals and dotted receivers. We also assumed the dotted place of defect. It is necessary to complete this algorithm with considering all real factors and influences for practice use.

Practical application of these algorithms will require the addition of defining areas of real fulfilment of the conditions of existence of the defect and it will need to analyse the effects of all factors on the accuracy of localization.

Acknowledgement

The work presented in this paper has been supported by the institutional development funding PRO K217.

References

- [1] VAN DEN ABEELE, KE.-A., JOHNSON, PA. and SUTIN, A. Nonlinear Elastic Wave Spectroscopy (NEWS) Techniques to Discern Material Damage, Part I: Nonlinear Wave Modulation Spectroscopy (NWMS). *Res Nondestr Eval*, 2000, vol. 12, no. 1, pp17-30. DOI: 10.1007/s001640000002.
- [2] HAJEK, K., KORENSKA, M. and SIKULA J. Nonlinear Ultrasonic Spectroscopy of Fired Roof Tiles, In *16th World Conference on Nondestructive Testing – Book of Abstracts*. Montreal, 2004, p. 42. [cited 2014-02-02]. Available from: <http://www.ndt.net/article/wcndt2004/pdf/materials_characterization/363_hajek.pdf>.

- [3] ZHAO, X., QI, X., ALEXANDER, S. and ABERNETHY, E. Damage Detection in Composite Cylinders Using Modulated Guided Wave Vibration. In *NDCM 2011*. Blacksburg, 2011. [cited 2014-02-02]. Available from: <<http://www.ndt.net/article/ndcm2011/papers/A-03-1.pdf>>.
- [4] PIECZONKA, L., STASZEWSKI, WJ., AYMERICH, F. and UHL, T. Analysis of Nonlinear Vibro-Acoustic Wave Modulations Used for Impact Damage Detection in Composite Structures, In *6th European Workshop on Structural Health Monitoring EWSHM 2012 – Materials and Qualification*. [cited 2014-02-02]. Available from: <<http://www.ndt.net/article/ewshm2012/papers/th2a2.pdf>>.
- [5] ZAITSEV, V., MATVEEV, L. and, MATVEEV, A. On the ultimate sensitivity of nonlinear modulation method of crack detection. *NDT&E International*, 2009, vol. 42, no. 7, p. 622-629.
- [6] SUTIN, AM. and JOHNSON, PA. Nonlinear elastic wave NDE II. Nonlinear wave modulation spectroscopy and nonlinear time reversed acoustics. In *Review of Progress in Quantitative Nondestructive Evaluation – AIP Conference Proceedings*. Melville: American Institute of Physics, 2005, p.385-392.
- [7] DOS SANTOS, S., VEJVODOVA, S. and PREVOROVSKY, Z. Nonlinear Elastic Wave Spectroscopy in Symbiosis with Time Reversal for Localization of Defects: Tr-News. In *5th International Workshop NDT in Progress*, Prague, 2009. [cited 2014-02-02]. Available from: <http://www.ndt.net/article/Prague2009/ndtip/proceedings/DosSantos_10.pdf>.
- [8] HÁJEK, K. and ŠIKULA, J. The New High Sensitive Variant of Nonlinear Ultrasound Spectroscopy for Nondestructive Testing. *Advances in Military Technology*, 2009, vol. 4, no. 1, p. 15-22.